Equilibrium free-energy differences at different temperatures from a single set of nonequilibrium transitions

Puneet Kumar Patra

Advanced Technology Development Center, Indian Institute of Technology Kharagpur, India

Baidurya Bhattacharya[*]

Department of Civil Engineering, Indian Institute of Technology Kharagpur, India

Crook's fluctuation theorem (CFT) and Jarzynski equality (JE) are effective tools for obtaining free-energy difference $\Delta F(\lambda_A \rightarrow \lambda_B, T_0)$ through a set of finite-time protocol driven nonequilibrium transitions between two equilibrium states A and B [parametrized by the time-varying protocol $\lambda(t)$] at the same temperature T_0. Using the generalized dimensionless work function ΔW_G, we extend CFT to transitions between two nonequilibrium steady states (NESSs) created by a thermal gradient. We show that it is possible, provided the period over which the transitions occur is sufficiently long, to obtain $\Delta F(\lambda_A \rightarrow \lambda_B, T_0)$ for *different* values of T_0, using the *same* set of finite-time transitions between these two NESSs. Our approach thus completely eliminates the need to make new samples for each new T_0. The generalized form of JE arises naturally as the average of the exponentiated ΔW_G. The results are demonstrated on two test cases: (i) a single particle quartic oscillator having a known closed form ΔF, and (ii) a one-dimensional ϕ^4 chain. Each system is sampled from the canonical distribution at an arbitrary T' with $\lambda = \lambda_A$, then subjected to a temperature gradient between its ends, and after steady state is reached, the protocol change $\lambda_A \rightarrow \lambda_B$ is effected in time τ, following which ΔW_G is computed. The reverse path likewise initiates in equilibrium at T' with $\lambda = \lambda_B$ and the protocol is time reversed leading to $\lambda = \lambda_A$ and the reverse ΔW_G. Our method is found to be more efficient than either JE or CFT when free-energy differences at multiple T_0's are required for the same system.

Consider a thermomechanical system whose equilibrium state is defined by its temperature T_0 and an external protocol λ fixed at λ_A (for example, the position of a confining potential [1], the position of the last molecule of a protein chain [2], etc.). A large class of problems in biological and chemical physics (such as transition between conformations of proteins, folding and unfolding of proteins, enzyme-ligand binding, hydration, etc.) concerns the change in free energy, $\Delta F(\lambda_A \rightarrow \lambda_B, T_0)$, of this system as its configurational space evolves under $\lambda(t)$ in a finite time τ corresponding to the final value $\lambda = \lambda_B$ and the system eventually relaxes to a new equilibrium at the same temperature T_0. Several methods have been proposed for computing $\Delta F(\lambda_A \rightarrow \lambda_B, T_0)$: thermodynamic integration [3], umbrella sampling [4], steered molecular dynamics [5], and nonequilibrium work relations [6–11].

The development of Jarzysnki's equality (JE) [6–8] and Crooks' fluctuation theorem (CFT) [9,10,12] has dramatically improved our ability to calculate free-energy differences [13–16] of real systems [2,17] through finite-time irreversible processes between two equilibrium states at the same temperature, T_0. Nevertheless, the task remains daunting because of the requirement of extensive sampling of the configurational space. In addition, $\Delta F(\lambda_A \rightarrow \lambda_B, T_0)$ thus computed is valid only for the particular temperature at which the samplings are performed, and if $\Delta F(\lambda_A \rightarrow \lambda_B, T' \neq T_0)$ is needed, then resampling of the entire data set is necessary at T'.

In this work we generalize CFT and JE by proposing a new fluctuation relation that enables us to calculate $\Delta F(\lambda_A \rightarrow \lambda_B, T_0)$ with good accuracy for a range of T_0 values using *a single set of sampling data*, thereby completely eliminating the need to generate new samples for each new T_0. The proposed fluctuation relation utilizes the transition between two nonequilibrium steady states, and T_0 features in the equation as a scaling parameter.

Let us now look at details of the problem. For a system in canonical equilibrium, the Helmholtz free energy is

$$F(T_0, \lambda) = -k_B T_0 \ln \left(\int \exp\left[-\beta_0 E(\Gamma, \lambda) \right] d\Gamma \right), \quad (1)$$

where k_B is the Boltzmann constant and $\beta_0 = (k_B T_0)^{-1}$. The system's energy $E(\Gamma, \lambda)$ depends upon the microstate Γ and varies parametrically over time according to $E(\Gamma(t), \lambda(t)) = \sum p_i^2/2m + \Phi(x_1, x_2, \ldots, x_N, \lambda(t))$, where p_i and x_i are the momentum and the position of the ith particle, and $\Phi(\cdots)$ is the potential energy of the system. In CFT, the system is initially in equilibrium state A with $\lambda = \lambda_A$. At time $t = 0$, λ starts to evolve until $t = \tau$, and stays fixed at its new value λ_B. During this period work $W^F = \int_0^\tau \dot{\lambda} \partial E/\partial \lambda \, dt$ is performed. The superscript F denotes the forward transition $A \rightarrow B$. Over time, the system relaxes to a new equilibrium state B with $\lambda = \lambda_B$. Being irreversible, the work W^F depends upon the initial microstate $\Gamma(0)$ of the system (and its surroundings), and therefore, an exhaustive sampling of the initial microstates provides the probability density of forward work, $P(W^F = w)$. Now consider the same system evolving in a reverse manner. The system begins at equilibrium state B where $\lambda = \lambda_B$, and over $0 \leqslant t \leqslant \tau$, λ traces itself back from $\lambda_B \rightarrow \lambda_A$. Eventually the system reaches the equilibrium state A. Repeated sampling of this reverse transition provides

---
[*]baidurya@civil.iitkgp.ernet.in

$P(W^R = -w)$ for the reverse work. CFT relates the ratio of these two densities with $\Delta F(\lambda_A \rightarrow \lambda_B, T_0)$:

$$\frac{P(W^F = w_0)}{P(W^R = -w_0)} = \exp\{-\beta_0[w_0 - \Delta F(T_0, \lambda)]\}. \quad (2)$$

The validity of (2) requires the dynamics to be ergodically consistent, i.e., if and only if a microstate has a nonzero probability in equilibrium state A, it evolves to a microstate that has a nonzero probability in equilibrium state B. Integrating (2) gives JE [18]. However, since T_0 is implicit in the sampling dynamics, the probability densities obtained cannot be used to calculate $\Delta F(T', \lambda)$ if $T' \neq T_0$. In order to employ a single set of sampling data for calculating $\Delta F(T', \lambda)$ corresponding to a range of temperature T', the dependence of sampling data on T_0 must be removed. We set out to do this by looking at the cumulative work and heat exchange during the *transition between two nonequilibrium steady states*.

Rather than beginning at equilibrium, we begin at a nonequilibrium steady state SS_1 obtained by imposing a temperature difference $(T_H - T_C)$ at the two ends of the conductor, where T_H and T_C are the temperatures of the hot and cold ends. This steady state originated from some primordial arbitrary equilibrium state A characterized by λ_A and T_0 by employing suitable temperature constraints. For all practical purposes, the system reaches a steady state when the relevant time-averaged macroscopic observables become stationary. T_H, T_C, and T_0 are related to each other through $T_H = T_0 + \Delta T_H$ and $T_C = T_0 - \Delta T_C$. Thus, depending upon ΔT_H and ΔT_C, the two not necessarily being equal, one can think of starting from arbitrarily different canonical equilibrium states. Note that this allows us to choose any arbitrary T_0.

After SS_1 is achieved, at $t = 0$, λ starts to evolve from λ_A until time $t = \tau$ when $\lambda = \lambda_B$ and work is performed. This external work does not result in any phase-space compression. Given sufficient time, the system reaches a new steady state SS_2. Upon removing the temperature constraints and bringing both ends in contact with T_0, the system eventually reaches the equilibrium state B, defined by λ_B and T_0. The reverse transition can likewise be accomplished under the time-reversed protocol. Such transition between steady states has been studied before in a different context [19]. The underlying principle governing our approach is the relaxation of a nonequilibrium state to an equilibrium state [20].

In state A (state B), the system follows the canonical distribution parametrized by λ_A (by λ_B):

$$f_{\text{eq},A}(\Gamma) = \frac{1}{Z_{\lambda_A}} \exp[-\beta_0 E(\Gamma, \lambda_A)]. \quad (3)$$

The density function of the nonequilibrium state and the Jacobian are given by Liouville's equation [21]:

$$f_{SS_1}[\Gamma(t)] = f_{\text{eq},A}[\Gamma(0)] \exp\left\{-\int_0^t dt'[\Lambda_H(t') + \Lambda_C(t')]\right\},$$

$$d\Gamma(t) = d\Gamma(0) \exp\left\{\int_0^t dt'[\Lambda_H(t') + \Lambda_C(t')]\right\}, \quad (4)$$

where $\Lambda = [\partial\dot{\Gamma}/\partial\Gamma]$ denotes the phase-space compression factor, with H (C) denoting the hot (cold) region. The intermediate region does not contribute to Λ (owing to

Hamilton's equation of motion). The normalizing constant corresponding to SS_1 is the same as the partition function for A. The phase-space compression factors are related to the heat flow [22–25] from the thermostats through

$$\langle\dot{Q}_H\rangle_t = k_B T_H \langle\Lambda_H\rangle_t t, \qquad \langle\dot{Q}_C\rangle_t = k_B T_C \langle\Lambda_C\rangle_t t. \quad (5)$$

Here $\langle\cdots\rangle_t$ denotes the time-averaged quantities. For the sake of compactness, we will drop t from the density functions and cumulative heat flows later. Next, we bring the generalized dimensionless time-integrated work function, $\Delta W_G(t)$ [26], into the picture, which can relate two microstates [$\Gamma(0)$ and $\Gamma(t)$], neither of them necessarily in equilibrium:

$$\exp[\Delta W_G(t)] = \frac{f_1[\Gamma(0)]d\Gamma(0)Z_{\lambda_0}}{f_2[\Gamma(t)]d\Gamma(t)Z_{\lambda_t}}. \quad (6)$$

The initial microstate $\Gamma(0)$ evolves to $\Gamma(t)$ in time t. $f_1[\Gamma(0)]$ (or $f_2[\Gamma(t)]$) is the probability density of $\Gamma(0)$ [or $\Gamma(t)$] corresponding to an associated equilibrium state 1 (or 2). We conjecture that such an association is possible after the system undergoing nonequilibrium transition loses its memory. Z_{λ_i} denotes the partition function at λ_i. Now we bring the superscripts F (for the forward transition $A \rightarrow SS_1 \rightarrow SS_2 \rightarrow B$) and R (for the reverse transition $B \rightarrow SS_2 \rightarrow SS_1 \rightarrow A$). The forward transition takes $\Gamma(0) \rightarrow \Gamma(t)$, while the reverse transition takes $\Gamma^*(0) \rightarrow \Gamma^*(t)$, where $\Gamma^*(0)$ is related to $\Gamma(t)$ through time-reversal mapping. The generalized work function during $A \rightarrow SS_1$ is (see Sec. I of the Supplemental Material [27])

$$\Delta W_{G,A\rightarrow SS_1}^F = \frac{1}{T_0}\int_0^t\left[\frac{\Delta T_H}{T_H}\dot{Q}_H^F - \frac{\Delta T_C}{T_C}\dot{Q}_C^F\right]dt'. \quad (7)$$

Proceeding analogously (see Sec. III of the Supplemental Material), the generalized work function during $A \rightarrow SS_2$ is

$$\Delta W_{G,A\rightarrow SS_2}^F = \frac{1}{T_0}\int_0^{t+\tau}\left[\frac{\Delta T_H}{T_H}\dot{Q}_H^F - \frac{\Delta T_C}{T_C}\dot{Q}_C^F + \dot{W}^F\right]dt'. \quad (8)$$

Therefore, the work function during $SS_1 \rightarrow SS_2$ can be obtained by subtracting (7) from (8):

$$\Delta W_{G,SS_1\rightarrow SS_2}^F = \beta_0 W^F + \frac{1}{T_0}\left[\frac{\Delta T_H}{T_H}Q_{H,\tau}^F - \frac{\Delta T_C}{T_C}Q_{C,\tau}^F\right], \quad (9)$$

where the heat flows are for the time duration τ over which λ changes. In a similar manner, we can compute the work function during the reverse transition $SS_2 \rightarrow SS_1$:

$$\Delta W_{G,SS_2\rightarrow SS_1}^R = \beta_0 W^R + \frac{1}{T_0}\left[\frac{\Delta T_H}{T_H}Q_{H,\tau}^R - \frac{\Delta T_C}{T_C}Q_{C,\tau}^R\right], \quad (10)$$

Now we make the important assumption of the ergodic consistency being valid during the transition $SS_1 \rightarrow SS_2$, and therefore, using (6) we can write

$$\exp[\Delta W_{G,SS_1\rightarrow SS_2}^F] = \frac{f_{\text{eq},A}[\Gamma_{SS_1}(0)]d\Gamma_{SS_1}(0)Z_{\lambda_A}}{f_{\text{eq},B}[\Gamma_{SS_2}(\tau)]d\Gamma_{SS_2}(\tau)Z_{\lambda_B}}. \quad (11)$$

The subscripts SS_i emphasize that the points are on trajectories whose evolution is described by equations of motion

that take the ensemble of states from SS_1 at 0 to SS_2 at τ. Because of the deterministic nature of the dynamics, $\Delta W^F_{G,SS_1 \to SS_2} = -\Delta W^R_{G,SS_2 \to SS_1}$. For simplicity, we now drop all subscripts except G. Assuming that the differences between the equilibrium density and the initial density under thermal gradient can be ignored for large τ, the probability densities of the forward and reverse work functions can be related as (12) (similar to as shown in Sec. III of the Supplemental Material):

$$P\big[\Delta W^R_G = -k\big] = e^{-k}\frac{Z_{\lambda_A}}{Z_{\lambda_B}}P\big[\Delta W^F_G = k\big]. \qquad (12)$$

A rearrangement results in the *proposed fluctuation relation*:

$$\frac{P\left\{\beta_0 W^F + \beta_0\left[\dfrac{\Delta T_H}{T_H}Q^F_H - \dfrac{\Delta T_C}{T_C}Q^F_C\right] = k\right\}}{P\left\{\beta_0 W^R + \beta_0\left[\dfrac{\Delta T_H}{T_H}Q^R_H - \dfrac{\Delta T_C}{T_C}Q^R_C\right] = -k\right\}} = e^{[k-\beta_0\Delta F]}, \qquad (13)$$

which is the main result of this Rapid Communication (henceforth, referred to as GCFR). Since the samplings are performed at T_H and T_C, the effect of T_0 is *inherently absent* in them, and β_0 is simply a scaling parameter. Depending upon the temperature at which ΔF is to be calculated, we can compute the forward and reverse densities of the work function simply by substituting the desired value of T_0. The generalized JE may be obtained by averaging:

$$\Big\langle e^{\{-\beta_0 W^F - \beta_0[(\Delta T_H/T_H)Q^F_H - (\Delta T_C/T_C)Q^F_C]\}}\Big\rangle = e^{-\beta_0\Delta F}. \qquad (14)$$

A second law type inequality can be recovered by applying Jensen's inequality to (14):

$$\langle W^F \rangle + \big\langle Q^F_H \big\rangle\frac{\Delta T_H}{T_H} - \big\langle Q^F_C \big\rangle\frac{\Delta T_C}{T_C} \geqslant \Delta F. \qquad (15)$$

We reiterate that Eqs. (12)–(15) are *not* exact relationships, and hold true *only* for large τ. Taking τ large enough, while fixing the time required to reach the steady state, ensures that the contributions arising from phase-space compressions become negligible.

We now test the effectiveness of (13) on a one-dimensional ϕ^4 chain of N particles. Its energy function is

$$E = \sum_{i=1}^{N}\frac{p_i^2}{2m_i} + \sum_{i=1}^{N-1}U(x_i,x_{i+1}) + \sum_{i=1}^{N}V(x_i). \qquad (16)$$

Here $U(x_i,x_{i+1}) = 0.5k_1(|x_{i+1} - x_i| - d)^2$ represents the quadratic nearest neighbor interparticle interaction, while $V(x_i) = 0.25k_2(x_i - x_{i,0})^4$ represents the quartic tethering potential with $x_{i,0}$ being the equilibrium position of the ith particle. We have kept $k_1 = 1.0$ and $m_i = 1.0$. k_2 plays the role of λ:

$$\begin{aligned}k_2 &= 0.25 && \forall\, t < 0\\ &= 0.25(1 + 10t/\tau) && \forall\, 0 < t \leqslant \tau\\ &= 2.75 && \forall\, t > \tau.\end{aligned} \qquad (17)$$

Test case 1. The first test case involves a single particle system (subscript 1 dropped) having a known analytical
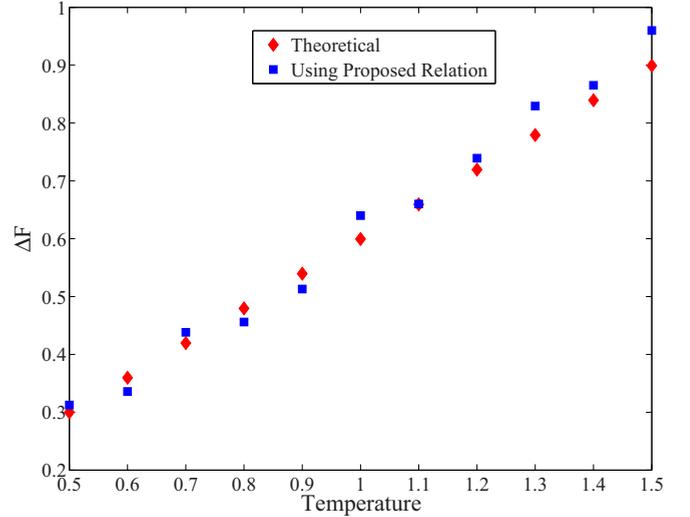

FIG. 1. Comparison of ΔF obtained using theoretical and proposed approaches in test case 1. Notice, that the proposed approach provides a good approximation to the theoretical results.

solution for ΔF:

$$\begin{aligned}\Delta F &= -k_B T_0 \ln\left(\frac{\int e^{[-\beta_0 11x^4/4]}e^{[-\beta_0 p^2/2]}dxdp}{\int e^{[-\beta_0 x^4/4]}e^{[-\beta_0 p^2/2]}dxdp}\right)\\ &= k_B T_0/4 \ln(11).\end{aligned} \qquad (18)$$

We compare this known ΔF with our results. We subject the single quartic oscillator to a position-dependent temperature field,

$$T(x) = 1 + 0.1\tanh(x), \qquad (19)$$

to bring it away from equilibrium. Temperature is controlled by a Hoover-Holian thermostat [28]. The system is simulated for 100 000 time steps (each time step $= 0.001$) under this temperature field through which it reaches SS_1. k_2 is changed over the next $\tau = 10\,000$ time steps according to Eq. (17). ΔW_G in this case is

$$\Delta W_G = \beta_0 W + \beta_0\int_0^\tau \dot{Q}dt' - \int_0^\tau \beta(x)\dot{Q}dt', \qquad (20)$$

where $\beta(x) = 1/k_B T(x)$ and $\dot{Q} = -\eta T(x) - 3p^2\xi T(x)$. η and ξ are the Hoover-Holian thermostat variables. $W = \mathcal{H}(\tau) - \mathcal{H}(0)$, where $\mathcal{H}(t) = p^2/2 + V + \int[\eta T(x) + 3p^2\xi T(x)]dt'$. Probability densities of generalized work are constructed using 60 000 random initial points. Figure 1 shows ΔF due to the evolution of k_2 as a function of temperature: GCFR is able to reproduce the theoretical results accurately for a range of temperatures without the need to resample at every new T_0.

Test case 2. We now consider a larger system ($N = 25$). The system is initialized with $x_i = x_{i,0} = i$ and random particle velocities. The equations are integrated using the classic Runge-Kutta algorithm with an incremental time step of 0.01. Post initialization, a temperature gradient is imposed on the system by keeping the two end particles at T_H and T_C using two Nosé-Hoover (NH) thermostats [29]. Subsequently, after 1×10^6 time steps (steady state is assumed to have
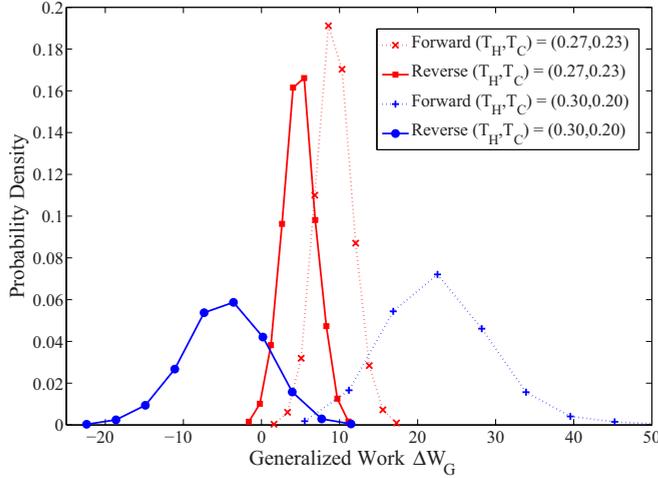
FIG. 2. Forward and reverse probability densities of generalized work function at $T_0 = 0.29$ calculated using 5000 forward and reverse trajectories using two sets of (T_H, T_C): (red) = (0.27, 0.23) and (green) = (0.30, 0.20). The intersection of forward and reverse ΔW_G densities gives ΔF, and is not affected by the choice of T_H, T_C. ΔF calculated using proposed fluctuation relation compares well with that of JE and CFT. Results obtained using the same data set for other T_0 values are similar, and agree well with CFT.

been reached), k_2 is made to evolve in $\tau = 100\,000$ time steps. The cumulative heat flow from the hot thermostat is $Q_H = -\int_0^t T_H \eta_H dt'$ (likewise for the cold), where $\eta_H(\eta_C)$ is the hot (cold) NH variable. The work done due to the change in tethering potential during time τ is $W = \mathcal{H}(\tau) - \mathcal{H}(0)$ where

$$\mathcal{H}(t) = \sum \frac{p_i^2}{2} + \Phi + \int_0^t \eta_C p_C^2 dt' + \int \eta_H p_H^2 dt'. \quad (21)$$

Here p_H (p_C) denotes the hot (cold) particle's momentum, and $\Phi = \sum U + \sum V$. ΔW_G^F and ΔW_G^R are sampled using 5000 trajectories each. Figure 2 shows probability densities of the forward and reverse generalized work functions $P(\Delta W_G^F)$ and $P(\Delta W_G^R)$ at $T_0 = 0.29$. Two pairs of (T_H, T_C)—red for (0.27, 0.23) and blue for (0.30, 0.20)—are chosen. The points of intersection of the forward-reverse pair gives $\beta_0 \Delta F$ (13) which should be independent of (T_H, T_C) for the same T_0 as evident from the figure. Importantly, these same 10 000 samples can be used to compute ΔF at *any* T_0. Table I shows

TABLE I. Comparison of free-energy differences using JE, CFT, and GCFR for seven different values of T_0. GCFR results are for two different steady states: $T_H = 0.27, T_C = 0.23$ and $T_H = 0.30, T_C = 0.20$. Notice that the ΔF obtained using GCFR matches closely with those from JE and CFT. It is interesting to note that the case of $T_H = 0.27, T_C = 0.23$ is able to approximate the equilibrium free-energy differences even for the states as far as $T_0 = 0.21$ and $T_0 = 0.29$. The results indicate that one can use a single set of data obtained during a transition between two NESSs and employ GCFR to calculate free-energy differences for a range of temperatures.

T_0	JE	CFT	GCFR $(T_H, T_C) = (0.30, 0.20)$	GCFR $(T_H, T_C) = (0.27, 0.23)$
0.21	1.39	1.35	1.40	1.39
0.22	1.48	1.50	1.49	1.46
0.24	1.64	1.60	1.67	1.62
0.25	1.73	1.70	1.75	1.69
0.26	1.81	1.79	1.83	1.78
0.28	1.98	1.97	2.02	1.97
0.29	2.07	2.00	2.10	2.07

seven such T_0 values, computed using both sets of (T_H, T_C). Not only is ΔF at a given T_0 independent of (T_H, T_C) as it should be, it is clear that T_0 does not even need to be within the range of (T_H, T_C) for the method to work.

Finally, Table I lists ΔF computed using JE and CFT at the seven different temperatures. While GCFR is able to identify ΔF as accurately as CFT and JE, it does so with only one set of samples. CFT and JE would require a new set of samples for each T_0, thereby imposing a severe computational or experimental burden on the analyst. As stated above, these transitions need to be carried out slowly. Our efforts to calculate ΔF using only $\tau = 100$ steps did not yield ΔF values commensurate with those shown in Table I.

To summarize, in this work generalized versions of CFT and JE have been presented. The proposed extensions present a suitable method through which equilibrium free-energy differences can be extracted from the information embedded within the nonequilibrium steady states. The augmented equations bear a remarkable similarity with those of CFT and JE with additional contributions arising due to heat flowing from the reservoirs. GCFR has been tested using two different cases, with each of them suggesting that GCFR is a suitable alternative to CFT and JE when evaluating ΔF at multiple temperatures.

[1] F. Mondaini and L. Moriconi, Phys. Lett. A **378**, 1767 (2014).

[2] D. Collin, F. Ritort, C. Jarzynski, S. B. Smith, I. Tinoco, and C. Bustamante, Nature (London) **437**, 231 (2005).

[3] J. G. Kirkwood, J. Chem. Phys. **3**, 300 (1935).

[4] G. Torrie and J. Valleau, J. Comput. Phys. **23**, 187 (1977).

[5] S. Park, F. Khalili-Araghi, E. Tajkhorshid, and K. Schulten, J. Chem. Phys. **119**, 3559 (2003).

[6] C. Jarzynski, Phys. Rev. Lett. **78**, 2690 (1997).

[7] C. Jarzynski, Phys. Rev. E **56**, 5018 (1997).

[8] C. Jarzynski, C. R. Phys. **8**, 495 (2007).

[9] G. E. Crooks, J. Stat. Phys. **90**, 1481 (1998).

[10] G. E. Crooks, Phys. Rev. E **60**, 2721 (1999).

[11] T. Hatano, Phys. Rev. E **60**, R5017 (1999).

[12] J. Horowitz and C. Jarzynski, J. Stat. Mech.: Theory Exp. (2007) P11002.

[13] D. A. Hendrix and C. Jarzynski, J. Chem. Phys. **114**, 5974 (2001).

[14] F. M. Ytreberg, R. H. Swendsen, and D. M. Zuckerman, J. Chem. Phys. **125**, 184114 (2006).

[15] H. Híjar, J. Quintana-H, and G. Sutmann, J. Stat. Mech.: Theory Exp. (2008) P05009.

[16] C. Dellago and G. Hummer, Entropy **16**, 41 (2013).

[17] J. Liphardt, S. Dumont, S. B. Smith, I. Tinoco, and C. Bustamante, Science **296**, 1832 (2002).

[18] D. J. Evans, Mol. Phys. **101**, 1551 (2003).

[19] S. Lahiri and A. M. Jayannavar, Eur. Phys. J. B **87**, 141 (2014).

[20] D. J. Evans, D. J. Searles, and S. R. Williams, J. Stat. Mech.: Theory Exp. (2009) P07029.

[21] D. J. Searles and D. J. Evans, Int. J. Thermophys. **22**, 123 (2001).

[22] J. N. Bright, D. J. Evans, and D. J. Searles, J. Chem. Phys. **122**, 194106 (2005).

[23] P. K. Patra and B. Bhattacharya, J. Chem. Phys. **142**, 194103 (2015).

[24] P. K. Patra and B. Bhattacharya, Phys. Rev. E **93**, 033308 (2016).

[25] P. K. Patra, W. G. Hoover, C. G. Hoover, and J. C. Sprott, Int. J. Bifurcation Chaos **26**, 1650089 (2016).

[26] S. R. Williams, D. J. Searles, and D. J. Evans, Phys. Rev. Lett. **100**, 250601 (2008).

[27] See Supplemental Material at http://link.aps.org/supplemental/ 10.1103/PhysRevE.94.040101 for the detailed derivation of the proposed relation.

[28] W. G. Hoover and B. L. Holian, Phys. Lett. A **211**, 253 (1996).

[29] W. G. Hoover, Phys. Rev. A **31**, 1695 (1985).